Contents lists available at ScienceDirect

Food Chemistry: Molecular Sciences

Peptides derived from the gastrointestinal digestion of amaranth 11S globulin: Structure and antioxidant functionality

Susan García Fillería [a],[1],[2], Agustina Estefania Nardo [a],[1],[3], Margot Paulino [b],[3], Valeria Tironi [a],[b],[*],[2]

[a] *Laboratorio de Investigación, Desarrollo e innovación en Proteínas Alimentarias (LIDiPA), Centro de Investigación y Desarrollo en Criotecnología de Alimentos (CIDCA-CCT La Plata-CONICET, CICPBA, Facultad de Ciencias Exactas, Universidad Nacional de La Plata), La Plata, Argentina*
[b] *Centro de Bioinformática Estructural (CeBioInfo), Departamento de Experimentación y Teoría de la Estructura de la Materia y sus Aplicaciones, Facultad de Química, Universidad de la República, Montevideo, Uruguay*

ABSTRACT

The relationship between structural and physicochemical properties and antioxidant activity of peptides from amaranth 11S-globulin was studied. Peptides AWEEREQGSR, TEVWDSNEQ, IYIEQGNGITGM and YLAGKPQQEH had the greatest *in vitro* activity (ORAC, HORAC). GDRFQDQHQ, HVIKPPSRA and KFNRPETT were the most active ones against Cu^{+2}/H_2O_2-induced-LDL oxidation. In a cellular system (H_2O_2-induced-Caco2-TC7), TEVWDSNEQ, IYIEQGNGITGM, GDRFQDQHQ, LAGKPQQEHSGEHQ and KFNRPETT were the most effective in decreasing ROS, while the effects on SOD, GPx, and GSH were variable. To understand the structure–antioxidant activity relationships, the content of aromatic and acidic amino acids, the degree of hydrophobicity and the charge distribution on the accessible surface of peptides structures obtained by molecular dynamics were analysed. The low correlation between *in vitro*, *ex vivo* and cellular activities could be explained by the influence of physicochemical and structural properties on the interaction with complex systems (LDL/cells), peptide modifications and/or mechanisms other than direct ROS inhibition in the cells.

1. Introduction

Peptides can act as antioxidants through different molecular mechanisms such as neutralisation of free radicals by direct electron transfer (SET) and hydrogen atom transfer (HAT) reactions, and reduction or chelating of pro-oxidant metals (Wen, Zhang, Zhang, Duan & Ma 2020; Zou, He, Li, Tang & Xia, 2016; Ketnawa, Wickramathilaka & Liceaga, 2018). Their antioxidant activity depends both on their amino acid composition and their length (number of residues), but also on their sequence, i.e. the location of specific amino acids in their chain (Gallego, Mora & Toldrá, 2018). The ability to form H-bridges, the electronic and hydrophobic properties of C- and N-terminal amino acids have been correlated with antioxidant capacity (Hernández-Ledesma, Amigo, Recio & Bartolomé, 2007). In addition, the structural properties and environment of certain residues in peptides are relevant in their

antioxidant potential (Nwachukwu & Aluko, 2019; Zou et al., 2016). For this reason, bioinformatics tools and, computational methods that allow modelling the three-dimensional structure of peptides and proteins have become highly relevant in the prediction of antioxidant activity and in the study of the underlying molecular mechanisms (Agyei & Udenigwe 2018). In addition, these methods are used to explore potential activity of peptides obtained from different protein sources and to establish relationships between structural properties and activities (Wen et al., 2020).

Cells have diverse complementary systems to prevent the oxidative damage including antioxidant enzymes and low molecular weight compounds capable to scavenge reactive oxygen species (ROS) such as reduced glutathione (GSH). When the balance between oxidation level and antioxidants in cells is altered, oxidative stress occurs. Antioxidant activity at cellular level could be exercised by direct mechanisms such as

ROS scavenging by SET or HAT and/or ROS formation inhibition by metal chelation. In addition, some substances function as inducers and/or cell signals that lead to changes in gene expression, which result in the activation of enzymes that individually or synergistically eliminate ROS (Finley, Kong, Hintze, Jeffery, Ji & Lei, 2011). To act like antioxidant, the peptides should be able to interact with or to penetrate the cell, being this property highly dependent on their physicochemical and structural characteristics (Wang, Wang, Huo & Li, 2016). Human adenocarcinoma cell line, Caco-2 and its clones have been widely used as an *in vitro* model for the small intestine and as a well-established model for investigating the antioxidant effect of bioactive compounds (Jiménez et al., 2016; O'Sullivan et al., 2012).

Amaranth proteins and derived peptides have different biological activities. Antithrombotic, antihypertensive, hypocholesterolemic, antiproliferative and, immunomodulatory activities have been demonstrated (Nardo, Suárez, Quiroga & Añón, 2020). Plant antioxidant peptides are of great interest for their potential use as nutraceuticals. In this sense, studies carried out in *Amaranthus* spp. underline the beneficial impact of hydrolysates and bioactive peptides as ROS scavengers and the influence of the molecular weight, structure, and amino acid composition (Park, Sharma & Lee, 2020). The antioxidant activity of simulated gastrointestinal digests of amaranth protein isolate and different fractions separated from it has been studied. *In vitro* ability to neutralize ROS (ROO•, OH•, ONOO–) and to chelate metals inhibiting the formation of OH• (Orsini Delgado, Galleano, Añón & Tironi, 2015), *ex vivo* prevention of the Cu^{+2}/H_2O_2-induced oxidation of LDL (García Fillería & Tironi, 2017), and intracellular activity (ROS inhibition, effects on GSH content and some enzymatic activities) (García Fillería & Tironi, 2021) have been proved.

However, the correlation between structure and activity is still not entirely clear for antioxidant peptides, since most studies focus on the identification and isolation of peptides. Given the structural diversity of peptides, it is to be expected that the same sequence can act as an antioxidant by different mechanisms. Moreover, it is important to study the bioavailability and the activity by different methodologies to evaluate their real potential biological action. In previous works, we have identified ten peptides (TEVWDSNEQ, IYIEQGNGITGM, GDRFQDQHQ, LAGKPQQEHSGEHQ, YLAGKPQQEH, PLQAEQDDR, HVIKPPSRA, AWEEREQGSR, AVNVDDPSK and KFNRPETT) generated from 11S globulin of amaranth seed by simulated gastrointestinal digestion with potential *in vitro* peroxyl radical scavenging activity, which was confirmed (ORAC assay) for some of them (Orsini Delgado, Nardo, Pavlovic, Rogniaux, Añón, & Tironi, 2016). The activity of these peptides against the Cu^{+2}/H_2O_2-induced oxidation of low-density lipoproteins (LDL) was also evaluated (García Fillería & Tironi, 2017). The objective of the present study was to correlate *in silico* characterization with *in vitro* acellular, *ex vivo* and cellular antioxidant activity of these amaranth peptides, evaluating potential structure–activity relationships and analysing the dependency of different antioxidant behaviours with the structural state and the interactions with lipoprotein particles or cells. For that, in addition to the measures previously done, *in vitro* antioxidant activity in aqueous solution by hydroxyl radical averting capacity (HORAC assay) and cell assays analysing different biomarkers were performed. In addition, potential modifications by cells and capability to cross an intestinal cell monolayer was evaluated. Besides, physicochemical properties (isoelectric point, charge, amino acid ratio and hydrophobicity/hydrophilicity ratio); peptide structure and properties derived from molecular dynamics simulations, and peptide-cell interaction properties were analysed by *in silico* methodologies.

2. Materials and methods

2.1. Materials and samples

Chemicals. 2′,7′-dichlorofluorescin diacetate (DCFH-DA), lysis buffer L6168, Superoxide dismutase determination kit 19160, Glutathione Peroxidase Cellular Activity Assay Kit CGP1, and Glutathione Assay Kit Fluorimetric CS1020 were purchased from Sigma Chemical Co. (St. Louis, MO, USA); hydrogen peroxide was from Rieder-del-Haën (Sigma-Aldrich, Seelze, Hannover, Germany). Dulbeccós modified Eagle medium (DMEM) and DMEM adhesion were from EMEVE (Medios de Laboratorio Microvel SRL, Buenos Aires, Argentina), heat-inactivated fetal calf serum (FCS) was from Internegocios SA (Mercedes, Buenos Aires, Argentina), penicillin/streptomycin (PenStrep), TrypLE Express and nonessential amino acids were from Gibco (Thermo Fisher Scientific, Waltham, MA, USA). All the other reagents were of analytical grade.

Peptides. In a previous work in our lab (Orsini Delgado et al., 2016), several peptides generated by simulated gastrointestinal digestion of amaranth 11S globulin were identified by LC-MS/MS in fractions with high activity measured by the ORAC method. Ten peptides were selected to be synthesized (Ontores Biotechnologies Inc., Shanghai, Shanghai, China) and further studied. Their sequences, localization in 11S globulin, and molecular weights are shown in Table 1.

2.2. In silico analysis

2.2.1. Physicochemical properties of peptides

Physicochemical properties such as isoelectric point, net charge, ratio of different types of amino acids, hydrophobicity/hydrophilicity ratio (GRAVY parameter, grand average hydropathy), were evaluated using the sequence manipulation suite server (http://www.bioinformatics.org/sms2/index.html) (Stothard, 2000).

2.2.2. Molecular dynamics and structural descriptors

The three-dimensional structure of each peptide was generated using the building tool of MOE2013.1 software (Molecular Operating Environment Version 2013.1, Chemical Computing Group). The structures were parametrized using the AMBER12 force field. Explicit solvation cubes with 6 Å margin using water and Na^+ and Cl^- as counter ions were built. The structures were minimized at 300 °K to a RMS gradient of 0.05 kcal/mol using periodic boundary conditions. Then, all structures were submitted to a 100 ps backbone restrained trajectories. Finally, molecular dynamics simulation of 4900 ps with the NTP microcanonical ensemble, without any restriction were carried out. The final 3D structure at 4900 ps simulation of each peptide was obtained. MOE suit was used to calculate i3D descriptors (which use relative 3D atomic coordinates). Volumes, accessible surface areas (ASA) and partition of this data as ASA^+ (considering strictly just atoms with $q_i > 0$, in which q_i is the partial charge of atoms), ASA^- (for all negatively charged atoms with $q_i \leq 0$), ASA_H (ASA of hydrophobic atoms, $|q_i| \leq 0.2$) and ASA_P (polar surfaces, $|q_i| \geq 0.2$) were obtained.

2.2.3. Interaction peptide-cell

Two parameters were evaluated:

- *Toxicity* was predicted through the ToxinPred server (http://crdd.osdd.net/raghava/toxinpred/index.html), which is designed to predict and design toxic or non-toxic peptides. This model is based on a significant number of toxic peptides ($1805 \leq 35$ residues) collected from various databases and it uses the machine-learning technique support vector machine (SVM) tool to discriminate toxic from non-toxic peptides (Gupta et al., 2013). These authors observed the presence of various motifs in the toxic peptides and that certain residues such as C, H, N and P are abundant and preferred in certain positions.

- *Cell penetration* was predicted through the CPPred server (http://distilldeep.ucd.ie/CPPpred). A peptide is considered capable of penetrating cells when the score is greater than 0.5, although a considerable percentage of false positives have been recorded taking this value (Holton et al., 2013).

Table 1
Sequence, localization and physicochemical properties of amaranth peptides.

Peptide	Sequence	Mr (Da)	Localization in globulin 11S	IP[1]	Charge (pH = 7)	% Amino acid						GRAVY[1]
						Hydrophobic uncharged	Acidic	Basic	Others	Aromatic	Sulfur	
P1	TEVWDSNEQ	1090.4679	35–43	3.42	−3.0	22.2	33.3	–	22.2	44.4	11.1	−1744
P2	IYIEQGNGITGM	1294.6227	74–86	3.85	−1.0	33.3	8.3	–	33.3	58.3	8.3	0.142
P3	GDRFQDQHQ	1129.4901	118–130	5.41	−0.9	11.1	22.2	22.2	11.1	44.4	11.1	−2533
P4	LAGKPQQEHSGEHQ	1544.7332	183–199	6.50	−0.8	21.4	14.3	21.4	21.4	42.9	–	−1814
P5	YLAGKPQQEH	1169.5829	235–242	7.54	0	30.0	10.0	20.0	30.0	40.0	10.0	−1530
P6	LQAEQDDR	973.4465	235–242	3.88	−2.0	25.0	37.5	12.5	25.0	25.0	–	−2050
P7	HVIKPPSRA	1003.5927	253–260	11.65	+2.1	55.6	–	33.3	55.6	11.1	–	−0.567
P8	AWEEREQGSR	1246.5690	260–269	4.48	−1.0	20.0	30.0	20.0	20.0	30.0	10.0	−2330
P9	AVNVDDPSK	943.4590	287–297	4.11	−1.0	44.4	22.2	11.1	44.4	22.2	–	−0.733
P10	KFNRPETT	991.5074	441–448	9.70	+1.0	25.0	12.5	25.0	25.0	37.5	12.5	−1950

Properties obtained from http://bioinformatics.org/sms2/protein_stats.html.
IP = isoelectric point.
Hydrophobic uncharged amino acids: F, Y, I, L, M, V, W, A.
Acid amino acids: D, E.
Basic amino acids: R, K, H.
Aromatic amino acids: F, W, Y.
Other amino acids: G, S, T, C, N, Q, P.
GRAVY (grand average of hydropathy): a score < 0 is related to a hydrophilic globular proteins, a score > 0 to a hydrophobic membrane protein, scores between −0.5 and 0.5 correspond to amphipathic proteins.

2.3. In vitro acellular antioxidant activity: hydroxyl radical averting capacity (HORAC)

The capacity of peptides to inhibit the formation of hydroxyl radicals by reaction of H_2O_2 and Co^{+2} was evaluated using fluorescein as an oxidizable fluorescent probe according to Orsini Delgado et al. (2015). Results were expressed as: OH• inhibition % = [(AUC$_S$ – AUC$_{NC}$) / (AUC$_B$ -AUC$_{NC}$)] × 100; where: AUC: area under curve; S: sample, B: blank (without H_2O_2/Co^{+2}), NC: negative control. Chlorogenic acid (0.05–0.50 g/L) was used as a reference compound. Measures were performed at least in triplicate.

2.4. In vitro cellular antioxidant activity

2.4.1. Cell cultures

Caco-2 TC7, a clone of the Caco-2 cell line with characteristics of ileum enterocitic cells with a high degree of morphological and functional differentiation (Turco, Catone, Caloni, Consiglio, Testai & Stammati, 2011) was used. Caco-2 TC7 (passages 39–40), from the American Type Culture Collection (ATCC) were thawed and cultured in DMEM supplemented with 15% w/v FCS, 4.5 g/L glucose, PenStrep (1000 UPen + 1000 ug/mL Strep), 13 mL/L), NaHCO$_3$ (2 g/L), gentamicin (0.5 g/L), 1% w/v non-essential amino acids, at pH = 7.4. Cell cultures were incubated at 37 °C in a humidified atmosphere containing 5% CO$_2$. In all trials, cells from no more than 9–10 subcultures were used.

2.4.2. Cytotoxicity of samples

2.5×10^4 cells/well were seeded onto 96 well plates and incubated (24 h, 37 °C, 5% CO$_2$). Cytotoxicity of samples was evaluated by the lactate dehydrogenase (LDH) assay. Leakage of LDH to the extracellular medium is an indication of damage to the cellular integrity. Solutions of the 10 peptides (1 mg/mL in 32.5 mM Na$_2$HPO$_4$/2.6 mM NaH$_2$PO$_4$, pH = 7.8 buffer) were analysed. Each well was incubated with 100 μL of sample for 3 h (37 °C, 5% CO$_2$). LDH activity was quantified in the supernatants by means of the LDH-P UV unitest kit (Wiener Lab, Rosario, Santa Fe, Argentina). Enzymatic activity was expressed as the absorbance (A) variation per min (ΔA/min, λ = 340 nm, SYNERGY HT-SIAFRT microplate reader, Biotek). Cytotoxicity was expressed as percentage compared to the cell death positive control (complete LDH release, DMEM with 3% Triton X-100 instead of sample).

The stressor cytotoxicity (500 μmol/L H$_2$O$_2$) was also determined by the LDH method.

2.4.3. Antioxidant activity of peptides

Intracellular ROS. The assay protocol was based on Ryu, Himaya, Qian, Lee & Kim (2011) with modifications. 2.5×10^4 cells/well were seeded in 96 wells plates and incubated (24 h, 37 °C, 5% CO$_2$). After medium removal and washing with PBS, 100 μL of 20 μmol/L DCFH-DA in PBS were added, incubating in dark for 30 min (37 °C, 5% CO$_2$). After DCFH-DA removal, 100 μL of sample were added. After incubation (1 h, 37 °C, 5% CO$_2$), sample removal, and washing with PBS, 100 μL of 500 μmol/L H$_2$O$_2$ was added. The mixture was incubated (37 °C) reading the fluorescence (λ_{exc} = 485 nm, λ_{em} = 528 nm, SYNERGY HT-SIAFRT) and the fluorescence value at 1 h was selected for the calculations. The following control systems were analysed: C1: maximum oxidation level (DCFH-DA, H$_2$O$_2$, no sample), C2: baseline (DCFH-DA, no sample, no H$_2$O$_2$), C3: intrinsic fluorescence (H$_2$O$_2$, no DCFH-DA, no sample). ROS inhibition % was calculated respect to C1 control as: (F$_{C1}$ - F$_S$) × 100 / F$_{C1}$ where F$_{C1}$: fluorescence of C1, and F$_S$: fluorescence in presence of sample.

2.4.4. Antioxidative enzymes and reduced glutathion (GSH) content

6.25×10^4 cells/well were seeded onto 48 wells plates and incubated (6 days, 37 °C, 5% CO$_2$). After removal of the medium, 200 μL of sample were added and incubated for 1 h (37 °C, 5% CO$_2$). Oxidation was induced with 200 μL of 500 μmol/L H$_2$O$_2$ in PBS (37 °C, 5% CO$_2$, 1 h). H$_2$O$_2$ was removed and cells were suspended with 200 μL of PBS, pelleted by centrifugation (600 xg, 5 min), and lysed (75 μL 1X lysis buffer, 15 min). After centrifugation (16000 xg, 10 min), the supernatant was stored at −80 °C. The superoxide dismutase (SOD) determination kit 19,160 was used to determine the SOD activity (% of inhibition of the rate of formazan formation, determined by decrease in absorbance (A) at 450 nm) using the following equation: SOD Activity % = [(A$_{blank}$ - A$_{sample}$) / (A$_{blank}$)] × 100, where blank was carried out with water instead of sample. Glutathione Peroxidase (GPx) Cellular Activity Assay Kit CGP1 was used in the determination of GPx activity (decrease of NADPH, A at 340 nm, ΔA/min), applying the following equation: GPx activity (mmol/min/mL = U/mL) = [(ΔA/min)$_{blank}$ - (ΔA/min)$_{sample}$]/ ε × b × V) where ΔA/min = (A$_{75s}$–A$_{15s}$)/60 s; ε × b = 3.6 mmol/L, V = sample volume (mL); blank was carried out with buffer instead of sample. For the determination of GSH, Glutathione Assay Kit Fluorimetric CS1020 was used; this is based on the formation of an adduct of monochlorobiman probe and GSH (λ_{exc} = 360 nm, λ_{em} = 460 nm). A calibration curve was performed with GSH (0.0–0.10 mmol/L). All results were expressed as percentage of C1, maximum oxidation control.

2.5. Passage and/or modification of samples by Caco-2 TC7 cells

The analysis was done in the apical-basolateral direction using polystyrene transwells Millicell-PIHP 01250 (Millipore, Burlington, MA, USA) with polycarbonate filter membranes (0.4 µm pore size, 12 mm diameter, 0.6 cm^2 effective area). The Caco-2 TC7 cells were seeded in the apical chamber (10^5 cells/cm^2) and incubated (37 °C, 5% CO$_2$) measuring the transepithelial electrical resistance (TEER) using a MillicellR-ERS (Millipore, Burlington, MA, USA) voltmeter for 20 days, when a constant value (TEER = 300 Ω.cm^2) was reached indicating the confluence of the monolayer. Then, 400 µL of sample was added to the apical chamber and 400 µL of PBS was added to the basolateral chamber and incubated for 3 h (37 °C, 5% CO$_2$). The original samples and those obtained after incubation were analysed with RP-HPLC using a Phenosphere Next C18 (5 µm 4.6 × 250 mm, Waters Corp., Milford, MA, USA) column. A linear gradient elution (0 to 100% of solvent B in A in 55 min) with a flow of 1.1 mL/min at 40 °C was applied; solvent A: water: acetonitrile (98:2), trifluoroacetic acid (TFA) (650 µL/L), solvent B: water:acetonitrile (35:65), TFA (650 µL/L). The injection volume was 200 µL.

2.6. Statistical analysis

Determinations were done in triplicate. One way-analysis of variance (ANOVA) was done. The Tukey Test was used for the multiple comparison of means with a significance level α = 0.05 (95% confidence) (GraphPad Prism version 5.0 software for Windows, GraphPad Software, San Diego, CA, USA).

3. Results

3.1. In silico analysis

3.1.1. Physicochemical properties of peptides

The activity of antioxidant peptides depends on both their physicochemical and structural properties. Table 1 summarizes the physicochemical properties of peptides under study: TEVWDSNEQ (P1), IYIEQGNGITGM (P2), GDRFQDQHQ (P3), LAGKPQQEHSGEHQ (P4), YLAGKPQQEH (P5), PLQAEQDDR (P6), HVIKPPSRA (P7), AWEEREQGSR (P8), AVNVDDPSK (P9) and KFNRPETT (P10). All peptides have molecular weights close to 1 kDa (8 to 14 amino acids) derive from the amaranth globulin 11S, an hexameric protein (300–360 kDa). Each monomer of 50–70 kDa contains an acidic (A, 27–37 kDa) and a basic (B, 20–24 kDa) subunits linked by a disulfide bond. Most of the identified derived peptide chains (P1 to P8) belong to the acidic subunit, while the sequences P9 and P10 belong to the end of the basic subunit (Table 1). High variability in the proportion of the different types of amino acids and in the isoelectric point (IP) values was observed. These results indicated that at the physiological pH (7.4), P7 and P10 will be cationic peptides; P5 will be neutral, while the rest of the peptides will be negatively charged. The GRAVY value for a peptide or protein could be calculated as the sum of hydropathy values of all amino acids according to the Kyte & Doolittle (1982) scale, divided by the number of residues in the sequence. For globular proteins, a strong correspondence between internal regions and GRAVY negative (hydrophobic) values and between external regions and GRAVY positive (hydrophilic) values has been observed. In the case of membrane-bound proteins, the portions of their sequences located within the lipid bilayer are correlated with hydrophobic areas. This parameter also has been used for the characterization of peptides (Bagag et al., 2013). Based on this, peptides with a GRAVY score below 0 will most likely be related to hydrophilic globular structures, while a score above 0 will most likely be in correspondence to a hydrophobic membrane-bound structure (Cid, Bunster, Canales & Gazitúa, 1992). According to Table 1, peptides P1, P3, P4, P5, P6, P8, and P10 showed strongly negative GRAVY values suggesting a high hydrophilic character. Meanwhile, P7 and P9 shown negative values but very

close to 0, and P2 showed a value just above 0 indicating a somewhat more hydrophobic character for these sequences, which could be characterized as amphipathic peptides.

3.1.2. Structure of peptides

Given that peptide antioxidant capacity could depend not only on the amino acid composition but also on the three-dimensional structure that it adopts, a prediction of their secondary and tertiary structure will be useful to understand this activity. It is generally accepted that short peptides (5 residues or less) adopt random coil conformations in aqueous solutions, but as the length of the chain increases, the formation of stable three-dimensional arrangements can modify the reactive properties of the different functional groups. The conformational spaces of peptides obtained by molecular dynamics were obtained according to the protocol above. With the objective to prove if trajectories reached the thermodynamic equilibrium, they were analysed by plotting the evolution of total energy (U) (Fig. S1, Supplementary Material Section). It could be concluded that all structures reached a thermodynamic equilibrium from the 500 ps, showing a collinear plot with respect to the time (x) axis. These final equilibrated structures are presented with their molecular surfaces coloured according to the electrostatic potential of the atoms. The electric atom surfaces are blue, red or white coloured, depending on their positive, negative or neutral electrostatic potential values, respectively. Alternatively, hydrophilic or lipophilic groups are pink or green coloured, respectively (Fig. S2, Supplementary Material Section). All the peptides exhibited mainly hydrophilic patches. However, some differences could be marked: P2 showed the highest proportion and distribution of hydrophobic zones on both sides, while P7 and P5 showed smaller hydrophobic zones. These visualizations agreed with the GRAVY parameter values (Table 1).

Molecular descriptors calculated based on the three-dimensional structure using the MOE software are shown in Table 2. P2, P3 and P4 presented the largest total solvent accessible surfaces area values (ASA). ASA could be partitioned in polar (ASA$_P$) and hydrophobic (ASA$_H$) surfaces. The ASA$_P$ could be expressed as the sum of ASA$^+$ and ASA$^-$. For P1, P6, P8, P9 and P10, ASA$_P$ was greater than ASA$_H$ having P8 the greatest ASA$_p$ value. P2 and P7 showed a higher proportion of exposed hydrophobic surface (ASA$_H$ greater than ASA$_P$). As regards peptide P7, presented the lower value of ASA$_P$ (mainly positive), the higher ASA$^+$ and the lower ASA$^-$ surfaces. Finally, the exposure degree to the solvent (grey scale in Fig. 1) depends on the amount of secondary structure of each peptide and concomitantly on the sequence length. In general, it could be conjectured that peptides of size like the ones under study here had flexible behaviour that is highly dependent on the environment in which they are located, with their R groups exposed to the solvent and could interact with other substances (free radicals, metals, etc.). The only exception could be P4, the largest one, which presented a tendency to form β-turn structures (Fig. 1B).

3.1.3. Peptide-cell interaction

Also some properties related to the peptide-cell interaction were studied using bioinformatics tools. The results obtained by using the ToxinPred server are shown in Table 3. According to this prediction, none of our peptides would be toxic. A parameter related to the cellular penetration capacity of the peptides was also analysed (*CCPred score)* and results are shown in Table 3. None of the peptides presented a high probability of cell penetration. P1, P2 and P3 have scores very close to 0 indicating that it is highly unlikely that they can penetrate a cell. P4, P5, P6 and P9 showed intermediate values within the present list, while P7, P8 and P10 had the highest scores and therefore would have the highest probability of cell penetration. In general, peptides capable of penetrating cells are considered to have lengths between 5 and 30 amino acids, are rich in basic amino acids that give them net positive charges, and have hydrophobic zones (Guidotti, Brambilla & Rossi, 2017, Holton et al., 2013). In our case, P7 and P10 show a net positive charge (Table 1), but P8 presents negative net charge. Its relatively high score

Table 2
Volume and accessible surface area to water (ASA) of peptides.

Peptide	Volume (Å^3)	ASA (Å^2)	Type of surface (% of total ASA)			
			Hydrophobic (ASA$_H$)	Polar (ASA$_P$)	Negative (ASA$^-$)	Positive (ASA$^+$)
P1	968.8	1440.6	45.2	54.8	49.3	50.7
P2	1194.5	1755.8	53.9	46.1	39.2	60.8
P3	1325.25	1872.8	46.8	53.2	35.9	64.1
P4	1389.1	1926.8	48.9	51.1	34.8	65.2
P5	1087.1	1567.2	51.9	48.2	33.9	66.2
P6	855.6	1346.4	41.6	58.4	45.6	54.4
P7	961.5	1504.5	56.3	43.7	23.9	76.1
P8	1109.2	1591.0	38.1	61,9	40.4	59.6
P9	748.6	1201.0	46.9	53.1	38.1	61.9
P10	920.9	1299.5	48.6	51.4	32.1	67.9

ASA: Water accessible surface area calculated using a radius of 1.4 A for the water molecule.
ASA$^+$: Water accessible surface area of all atoms with positive partial charge (strictly greater than 0).
ASA$^-$: Water accessible surface area of all atoms with negative partial charge (strictly less than 0).
ASA$_H$: Water accessible surface area of all hydrophobic ($|q_i| < 0.2$) atoms.
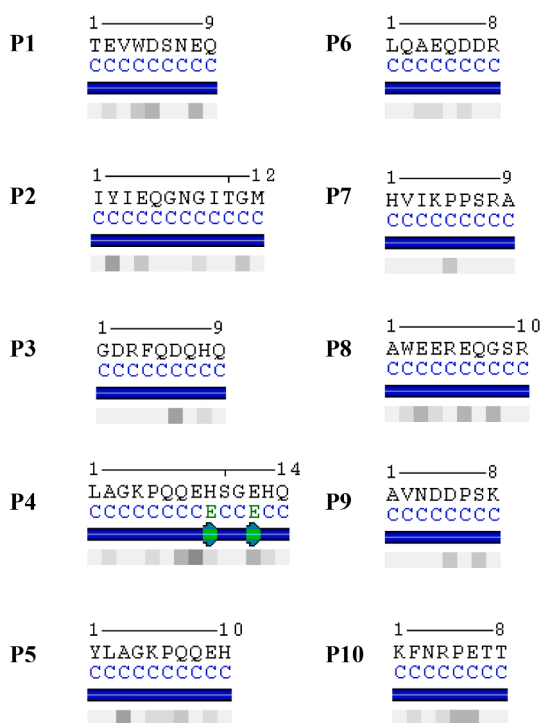ASA$_P$: Water accessible surface area of all polar ($|q_i| \geq 0.2$) atoms.

Fig. 1. Secondary structure of the final peptide conformations obtained by molecular dynamics. C (blue) = coil, E (green) = β turn or bridge. Solvent relative accessibility (RSA) is shown in grey scale: black = 0–9% RSA, white = 90–100% RSA (*http://polyview.cchmc.org/*). (For interpretation of the references to colour in this figure legend, the reader is referred to the web version of this article.)

suggests that it would behave like an amphipathic cell penetrating peptides (CPPs) since it contains both polar (hydrophilic) and nonpolar (hydrophobic) regions. P8 has two arginines, which are distributed throughout the sequence, and it is not especially rich in hydrophobic residues.

3.2. Antioxidant activity of peptides

Table 4 summarizes the antioxidant activities of amaranth peptides evaluated by different methodologies. According to our previous results peptide P8 presented the highest ORAC capacity (about 7 µg/mL neutralize the 50% of ROO•), followed by P5, P2 and P1 with comparable capacity (IC$_{50}$ values close to 20 µg/mL). P4 followed by P7 and

Table 3
Antioxidant activity of antioxidant peptides derived from the gastrointestinal digestion of amaranth proteins.

Peptide	ORAC IC$_{50}$ (mg/mL)	HORAC inhibition %	Inhibition of LDL oxidation	
			LT/LT$_C$ %	VP/VP$_C$ %
P1	0.020 ± 0.003	56 ± 6	122	101
P2	0.017 ± 0.003	66 ± 6	102	82
P3	0.6 ± 0.1	na	517	12
P4	0.14 ± 0.03	25 ± 2	186	31
P5	0.016 ± 0.03	57 ± 2	98	39
P6	na	23 ± 13	136	71
P7	0.57 ± 0.08	25 ± 5	nd	nd
P8	0.007 ± 0.001	79 ± 1	108	59
P9	na	15 ± 4	124	79
P10	na	na	247	18

ORAC: IC$_{50}$: 50 % inhibitory concentration was obtained from the dose–response curves fitting; na: no activity for concentrations up to 1 mg/ml (Orsini Delgado et al., 2016).
HORAC (0.2 mg/mL), na: no activity.
Inhibition of LDL oxidation. Kinetic parameters of conjugated diene evolution: LT = lag time in presence of peptides; LT$_C$ = lag time in maximum oxidation control; VP = Propagation rate in presence of peptides, VP$_C$ = Propagation rate in maximum oxidation control; nd: not determined since there was complete inhibition of oxidation (García Fillería & Tironi, 2017).

P3, showed significantly lower antioxidant capacities (between 6 and 90 times) than P8, while P6, P9 and P10 did not show activity by this method (Orsini Delgado et al., 2016). The evaluation through another assay in acellular systems (HORAC) was performed in the present work. Table 4 shows the OH• inhibition values (%) corresponding to peptide solutions (0.2 mg/mL). P8, P5, P2 and P1 exhibited the highest activities in the HORAC assay (between 56 and 79% inhibition). P4, P6 and P7 showed intermediate activity in HORAC assay. Finally, P3, P9, and P10 exhibited very little or no activity in the HORAC assay.

The capacity of the peptides (0.2 mg/mL solutions) to inhibit the Cu^{+2}/H$_2$O$_2$ induced lipid oxidation of human LDL was also included in Table 4. The most active peptides in this case were P7 which produced a complete inhibition of the lipid oxidation of the LDLs, followed by P3 and P10 which produced an important increase (about 5 and 2.5 times, respectively) of the lag time (LT) and diminution of the propagation rate (PR, 12 and 18% compared to the system without any peptide), and then P4, P6, P9 (moderate effects on both parameters). P8, P5, and P2 produced some effect only on the PR while P1 effected only on the LT of the LDL oxidation (García Fillería & Tironi, 2017).

Since our interest was to study the activity of peptides that were able to interact with and/or to enter cells, for cell assays, the sample was added first and, after incubation, the free sample was removed before

Table 4

Antioxidant activity of antioxidant peptides derived from the gastrointestinal digestion of amaranth proteins.

Peptide	ORAC IC$_{50}$ (mg/mL)	HORAC inhibition %	Inhibition of LDL oxidation	
			LT/LT$_C$ %	VP/VP$_C$ %
P1	0.020 ± 0.003	56 ± 6	122	101
P2	0.017 ± 0.003	66 ± 6	102	82
P3	0.6 ± 0.1	na	517	12
P4	0.14 ± 0.03	25 ± 2	186	31
P5	0.016 ± 0.03	57 ± 2	98	39
P6	na	23 ± 13	136	71
P7	0.57 ± 0.08	25 ± 5	nd	nd
P8	0.007 ± 0.001	79 ± 1	108	59
P9	na	15 ± 4	124	79
P10	na	na	247	18

ORAC: IC$_{50}$: 50 % inhibitory concentration was obtained from the dose–response curves fitting; na: no activity for concentrations up to 1 mg/ml (Orsini Delgado et al., 2016).

HORAC (0.2 mg/mL), na: no activity.

Inhibition of LDL oxidation. Kinetic parameters of conjugated diene evolution: LT = lag time in presence of peptides; LT$_C$ = lag time in maximum oxidation control; VP = Propagation rate in presence of peptides, VP$_C$ = Propagation rate in maximum oxidation control; nd: not determined since there was complete inhibition of oxidation (García Fillería & Tironi, 2017).

treatment with the stressor agent. Diverse assay conditions (cell density to be seeded, incubation time after seeding, order of sample and probe addition, concentration and time of treatment with the probe and with the sample, concentration of stressor) were previously optimized in our lab. Based on the cytotoxicity results and preliminary assays, incubation with 500 µmol/L H$_2$O$_2$ was selected as the oxidative stress inducer (García Fillería & Tironi, 2021).

Intracellular antioxidant activity can be measured by different bio-markers such as inhibition of ROS, biomolecules oxidation, activity of antioxidant enzymes, endogenous antioxidant molecules, expression of related genes and cell death (López-Alarcón & Denicola, 2013). Solutions of the 10 peptides at 1 mg/mL were analysed. Citotoxicity assay showed values of LDH leakage ≤10% for all the peptides, indicating that none of them produced significant cell damage. Based on preliminary assays, incubation with 500 µmol/L H$_2$O$_2$ was selected as the oxidative stress inducer. After 3 h of treatment, a low level of cellular integrity loss was observed by labelling with propidium iodide and flux cytometry and by LDH releasing (García Fillería & Tironi, 2021). Other studies showed that the cytotoxic effect of H$_2$O$_2$ on Caco-2 cells depended on the concentration and the time showing that concentrations at the mM level produced high (>50%) cytotoxicity (Cilla et al., 2018; Wang, Ding, Wang, Zhang, & Liu, 2015). Besides, the addition of 500 µmol/L H$_2$O$_2$ led to an increase of ROS during the entire incubation in our assay conditions (García Fillería & Tironi, 2021). This concentration has been previously used to generate oxidative stress in Caco-2 cells (Leong, Burritt, Hocquel, Penberthy, & Oey, 2017). As mentioned earlier, for intracellular antioxidant activity assays the sample was added first and, after incubation, the free sample was removed. After that, the stressor (500 µmol/L H$_2$O$_2$) was added.

Regarding the intracellular ROS assay, the analysis of the control systems showed that the treatment with 500 µmol/L H$_2$O$_2$ (1 h) produced a significant increment of ROS in Caco2-TC7 cells (Fig. S3, Supplementary Material Section). There was no development of non-specific fluorescence (C3); while C2 showed a fluorescence increase related to the endogenous ROS content of the cells (baseline) (Fig. S3A), with a ratio C2/C1 = 611 % after 1 h of incubation. In the presence of H$_2$O$_2$ (C1), a significant increment of fluorescence (1 h of incubation) compared to C3 (ratio C1/C3 = 1448 %) and compared to C2 (ratio C1/C2 = 206 %) were registered (Fig. S3). After treatment with amaranth peptides, the evolution of ROS presented different behaviours; in Fig. S3B two examples are shown. The content of ROS (% respect to C1) in cells pre-incubated with the different samples corresponding to t = 1 h

after the induction of oxidation is shown in Fig. 2A. P8 and P9 did not produce significant differences (p > 0.05) when compared to C1. On a different way, P1, P2, P3, P4, P7, and P10 presented a significant decrease (p < 0.05) in the intracellular content of ROS, without significant differences (p > 0.05) with C2, indicating that these six peptides managed to inhibit the formation and/or to scavenge ROS by keeping cells in the baseline oxidation state. These peptides achieved an inhibition of 32 to 42% (ROS content between 58 and 68% compared to C1). Differently, P5 and P6 produced a significant diminution (p < 0.05) of ROS content (21 and 22%, respectively), but it was not enough to return the cell to the baseline.

Regarding effects on intracellular antioxidants, GSH in C2 was significantly (p < 0.05) lower than in C1 (ratio C2/C1 = 71.5), indicating an increase of this endogenous antioxidant after H$_2$O$_2$ treatment. On the other hand, there were not changes in enzymatic activities, SOD and GPx (Fig. S4, Supplementary Material Section). According to previous studies, the enzymatic defence can be induced or consumed after treatment with a stressor, increasing or decreasing their level or activity, respectively. Results similar to those present have been previously reported by us and by other authors (García Fillería & Tironi, 2021). In addition, the SOD and GPx activities and the GSH content were evaluated in lysates of cells pre-incubated with the peptides and then treated with 500 µmol/L H$_2$O$_2$. Results of SOD activity are shown in Fig. 2B. The pre-treatment with P4 produced a significant decrease of SOD activity compared to C1 (p < 0.05), with no significant difference compared to C2. On the other way, cells pre-treated with P7 and P8 showed significantly (p < 0.05) higher values than C1 and C2. GPx activity (Fig. 2C) showed an important and significant decrease (p < 0.05) after pre-treatment with P6 and P8, with activity values of 25 and 37% compared to C1. Differently, P5 induced a significant increase in GPx activity compared to C1 (187%) and C2. Finally, Fig. 2D shows the results of the intracellular GSH content. Pre-incubation with seven of the peptides (P1, P2, P4, P5, P6, P8, and P9) led to a significant increase of GSH over C1 (p < 0.05). P1 and P2 were the ones that induced the greatest increases (almost 90%). In a different way, P3, P7 and P10 did not present significant differences (p > 0.05) compared to C1.

3.3. Simulated intestinal absorption and/or modification of peptides by cells

The intestinal lining was simulated by a monolayer of Caco-2 TC7 cells and the potential passage of the 10 peptides (1 mg/mL, 35 mmol/L phosphate buffer pH = 7.8) was evaluated. Untreated peptide solutions, apical and basolateral chambers after incubation (3 h), were analysed by RP-HPLC. As control, buffer samples were analysed in order to discriminate peaks that did not correspond to peptide samples. Various behaviours were recorded (Fig. S5, Supplementary Material) which could be classified into five groups: 1) No modifications in the apical chamber, the original peptide appeared in the basolateral chamber (P6, Fig. S5.A). 2) Partial modifications in the apical chamber (appearance of new components), no passage to basolateral chamber (P2, Fig. S5.B). 3) Partial modifications in the apical chamber (appearance of new components), both the original and the modified peptides were able to cross the monolayer appearing in the basolateral chamber (P3, P5, P8, and P9, Fig. S5.C and S5.D). 4) Partial modifications in the apical chamber (appearance of new components), only the original peptides managed to cross the monolayer and appear in the basolateral chamber (P4 and P10, Fig. S5.E). 5) Total modification in the apical chamber (disappearance of the original peptide and appearance of new components), passage of the new components to the basolateral chamber (P1 and P7, Fig. S3.F).

4. Discussion

Based on the described results, possible relationships between the physicochemical and structural properties of the peptides and their antioxidant activity in different environments can be analysed. The
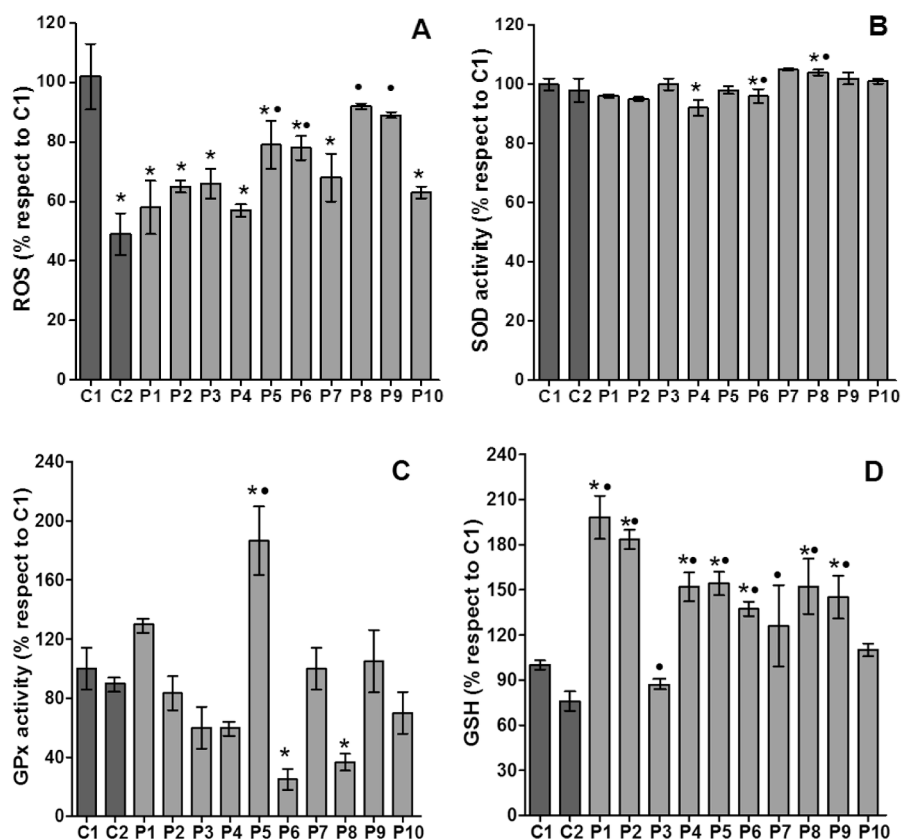
Fig. 2. Intracellular antioxidant activity of peptides solutions (1 mg/mL). Results are expressed as percentages compared to C1 (mean ± SD). Significant differences (p < 0.05) between peptides-treated cells and control cells (C1 and C2) are shown: * indicates significant differences compared to C1, ● indicates significant differences compared to C2. A: ROS content. B: Superoxide dismutase activity. C: Glutathione peroxidase activity. D: Reduced glutathione content.

antioxidant activity of amaranth peptides was evaluated by two *in vitro* chemical (acellular) assays: ORAC and HORAC. ORAC assay measures hydrophilic chain-breaking antioxidant capacity against ROO● radicals induced by 2,2′-Azobis(2-amidinopropane) dihydrochloride (AAPH), which proceed as a classic HAT mechanism; while HORAC assay shows mainly the capacity of the antioxidants to chelate metals inhibiting the formation of the OH● radicals. Although the ORAC and HORAC assays did not present completely comparable results, some similar behaviour could be observed. P8, P5, P2, and P1 were the most active peptides by both methods. These four peptides, all derived from the acid subunit of 11S globulin, have negative or neutral charge (Table 1). Two of them (P8 and P1) have a great proportion of acidic amino acids, while P5 and P2 have the higher proportion of hydrophobic amino acids. Within the group of the least active or non-active peptides (P3, P4, P6, P7, P9, and P10), differences between ORAC and HORAC activities were observed. In the simplest way to relate structure and bioactivity, we took into account the amino acid composition of each peptide to make several guesses. According to information found in the literature, the most active peptides (P8, P5, P2 and P1) have some aromatic amino acid (W or Y) in their sequence and at least one acidic amino acid (E or D) which can contribute to the antioxidant activity. In the case of P8, the presence of a charged amino acid (K) in the C-terminal position, with P and V in the second N-terminal position could also contribute to ORAC activity (Li & Li, 2013). Regarding the chelating activity of metals, the importance of the presence of E, D, H and K residues was demonstrated in fractions of rice bran protein; greater chelating activity was recorded as the content of H was higher (Phongthai, D'Amico, Schoenlechner, Homthawornchoo & Rawdkuen, 2018). As previously stated, the 4 most active peptides presented E; in addition, P1 contains D and P5 contains K and H. They also contained the amino acid Q. Increased chelating

activity due to the presence of a Q residue at the N-terminus have been reported since Q contains a carbamoyl group (–CONH2) in its structure, the carbonyl group (–CO) is able to function as a ligand facilitating the formation of a stable complex with the metal ion (Egusa Saiga & Nishimura, 2013). Hydrophobicity was reported to help to increase the antioxidant activity for pea-derived peptides (Pownall, Udenigwe & Aluko, 2010). Besides, when the linear sequence of each peptide is observed, the GRAVY parameter can help to understand the hydrophobicity and their variations and a putative relationship with the antioxidant activity. P2 is the only peptide that presents a hydrophobic character according to the GRAVY parameter and has the highest ASA$_H$. P1, P5 and P8 are hydrophilic in agreement with their proportion of ASA$_P$ (Table 1, Table 2 and Fig. S1).

Comparing ORAC and HORAC results with those obtained against Cu^{+2}/H$_2$O$_2$-induced LDL oxidation, peptides with the highest ORAC and HORAC activities (P8, P5, P2) mainly produced a reduction in the PR of lipid oxidation in LDLs (Table 4). However, peptides with the highest activity against Cu^{+2}/H$_2$O$_2$-induced oxidation of LDL (P7, P3 and P10) did not show high activity of ROO● scavenging (ORAC), even P10 did not register this activity. They also did not have significant HORAC activity; P3 and P10 did not show inhibition of OH● formation. Besides, these three peptides have diverse physicochemical properties (Table 1 and Table 2). P7 is a positively charged peptide that contains a high proportion of aliphatic and basic amino acids, with considerable hydrophobic character. P3 is a negatively charged peptide with a high proportion of acidic amino acids, is the most hydrophilic peptide of those analysed according to the GRAVY parameter and has a high ASA$_P$ to the solvent. P10 is a positively charged peptide, with no significant predominance of any type of amino acid, with hydrophilic character. The acidic peptides P1, P2, P6, P8 and P9 produced some slight effects

on the time of induction (LT) and/or on the PR of the lipid oxidation (conjugated diene formation) of LDLs (Table 4). Two of the most active peptides are cationic (P7 and P10), two of them (P7 and P3) have H, and two of them (P7 and P10) have K in their sequences, at different locations of the molecules. These results agree with the results presented by Wang et al. (2016) and Pan et al. (2019). On other hand, P7, P3 and P10 contain hydrophobic amino acids. Hydrophobic amino acids (e.g. L, P) are important to enhance the antioxidant properties of the peptides, since they can increase the accessibility of the antioxidant peptides to hydrophobic targets, such as LDL in this case. In this way, in addition to the presence of chelating or radical neutralizing amino acids such as H or aromatics, other structural characteristics could modify the ability of the peptides to interact with LDL particles in order to be able to prevent their oxidation. In agreement with this, hystidine-containing peptides showed differences in behaviour against LDL oxidation, and this behaviour did not directly correlate with the ability to capture peroxyl radicals (ORAC) or with the inhibition of the formation of OH• radicals by chelation (HORAC) measured in the systems where the peptides reacted directly (in aqueous solution) with these species. A possible explanation for these discrepancies could be that peptides establish interactions with the LDL surface, and that these interactions could induce conformational changes of peptides, exposing certain residues differently than they do in solution.

When Caco-2 TC7 cells were treated with amaranth peptides before the application of H_2O_2, various combinations of responses of the different parameters evaluated were recorded. We found that all peptides except P8 and P9 were able to reduce the intracellular ROS content (compared to the induced control system, C1), with some more active peptides (P1, P2, P3, P4, P7 and P10) that were able to keep the cells at their baseline ROS content. However, different effects on the activity of the antioxidant enzymes SOD and GPx and the content of GSH (no changes, decreases or increases) accompanied the decrease of ROS (Fig. 2), suggesting that different peptides were able to exert different cell actions. The decrease of ROS after pre-treatment with amaranth peptides could occur by different mechanisms: 1) Peptides could enter the cell and act as ROS scavengers inside the cell. 2) Peptides could enter the cell and produce some effect on signalling pathways that lead to induction of enzymes or antioxidant compounds. 3) Peptides could interact with the plasma membrane and induce signalling pathways that activate enzymes or antioxidant compounds. Similar behaviours (that is variability in the biomarkers responses) have been recorded when Caco2-TC7 cells were exposed to gastrointestinal digests of amaranth proteins and derived fractions under similar test conditions (García Fillería & Tironi, 2021) and, also with other peptides, other cell cultures and other tests conditions (Ryu et al., 2011; Wang et al., 2015; Wang et al., 2016; among others).

Results obtained in acellular systems, ORAC and HORAC assays, demonstrated that P6, P9 and P10 showed very little or no scavenging activity (Table 4). P9 was also unable to reduce the level of intracellular ROS. However, P6 and P10 produced a diminution of intracellular ROS. Furthermore, P8 (the most active in ORAC and HORAC assays) exhibited low or no intracellular activity. In other way, the most active peptides against LDL oxidation (P7, P3 and P10) were also able to decrease the ROS level to the basal state in cells. However, other peptides that produced the same effect on intracellular ROS (P1, P2, and P4) did not have very important effects on LDLs. The lack of correlation between cell and acellular assays could have different causes such as: 1) Peptides could experiment modifications by cell peptidases that could change the activity of the molecules; 2) The peptides could act by mechanisms other than direct inhibition of ROS in the cells. Lack of correlation between ORAC capacity and the ability to control intracellular oxidative stress of other food components has been demonstrated; an effect on the Nrf2 system has been verified in some cases (Finley et al., 2011). From our results, we could infer that some of the peptides could exert some indirect effects that were reflected in changes in SOD and GPx activities and in the GSH level. An effect registered for 7 of the 10 peptides was a

significant increase in the GSH content in comparison to the control of maximum oxidation (C1). However, five of these peptides corresponded to cases where ROS content was reduced to baseline levels and the other two were those that failed to decrease ROS (P8 and P9) (Fig. 2).

Potential modifications by and/or passage through the intestinal cells were evaluated. Analysing the chromatographic behaviour of the original peptides, their RP-HPLC retention times (RT) corresponded to a zone of intermediate hydrophobicity. Peptides that presented the highest RT (P2, P7) also registered a slightly hydrophobic GRAVY index (Table 1). The rest of them, with greater hydrophilic character according to GRAVY, presented lower RT but without a direct correlation between the two parameters, probably due to other factors that may influence the chromatographic behaviour, such as the molecular mass. Different behaviours were observed when peptides were in contact with the monolayer of Caco-2 TC7 cells that simulated the intestinal lining. Regarding the attack by peptidases of brush border, three performances were observed: total degradation, that is, total disappearance of the original peptide and appearance of hydrolysis products (P1 and P7); partial degradation in which the original peptide remained and hydrolysis products appeared (P2, P3, P4, P5, P8, P9 and P10); and a case where no modification of the original peptide was registered (P6). In most cases, the hydrolysis products were more hydrophilic than the original peptide (P1, P3, P4, P7, P8, P9 and P10) except for P5 whose products were more hydrophobic. Regarding the passage through cell monolayer, it was evident that in many cases there was transport to basolateral chamber of some of the products generated by the action of peptidases (P1, P3, P4, P5, P7, P8, and P9). Within cases where original peptide remained, P3, P5, P8 and P9 were also able to cross the monolayer in different proportions; P6 (which was not attacked by peptidases) managed to cross the cell monolayer. When transcellular transport through cells occurs, an attack by cytoplasmic peptidases could be possible (Azad & Wright, 2012). There is no evidence of this in any of the tests carried out in this work, since none of the basolateral chambers showed peaks that were not present in the corresponding apical chambers. However, some intracellular modification that generates new peptides with similar chromatographic properties cannot be ruled out. Regazzo et al. (2010) have shown that a β-casein fragment, which is a long and hydrophobic peptide (17 amino acids, 1881 Da) with immunomodulatory activity, could be absorbed mainly by transcytosis. These authors stated that it is very likely that it resisted hydrolysis thanks their content of P (YQEPVLGPVRGPFPIIV). Other authors have also shown that high proline-peptides were able to resist hydrolysis (Savoie, Agudelo, Gauthier, Marin & Pouliot, 2005). Quiros, Dávalos, Lasunción, Ramosa & Recio (2008) demonstrated that the antihypertensive pentapeptide, HLPLP, also derived from β-casein, is capable of being absorbed and remaining intact; in this case though the paracellular route. Therefore, there are various experimental evidences that show that peptides with >3 amino acids could be absorbed intact through intestinal epithelium, depending on several factors such as molecular mass, hydrophobicity, net charge or tendency to aggregate (Aito-Inoue, Lackeyram, Fan, & Sato, 2007). Xu et al. (2017) studied the absorption of a peptide derived from the rapeseed protein, YWDHNNPQIR (called RAP) using Caco-2 cell monolayers as a model. The results showed that a percentage of this peptide managed to pass intact through the monolayer while three main fragments (WDHNNPQIR, DHNNPQIR and YWDHNNPQ) and five modified RAP-derived peptides were found on both the apical and basolateral sides. In our work, proline-containing peptides were partially (P5 and P9) or totally degraded (P7) by extracellular peptidases. P6 (LQAEQDDR) which showed the greatest resistance to hydrolysis by extracellular peptidases, has R in C-terminal, like others previously reported (Xu et al., 2017), although we do not have information about the relevance of this fact to the resistance to brush border peptidases.

The peptides with the greatest effects in preventing Cu^{+2}/H_2O_2-induced LDL oxidation were P7, P3, and P10. Peptide P7 was completely degraded by brush border peptidases; P10 was partially degraded by

peptidases to more hydrophilic molecules and these were able to cross the cell monolayer but not the original molecule; P3 was partially degraded, and both the products generated and the remaining peptide could cross the monolayer. P6 and P9 were able to cross the intestinal cells without previous modifications and had a moderate activity against the oxidation of LDL (only oxidation propagation rate). P5 and P8 presented the same behaviour but with even less important activities. According to results presented, P3 emerged as the best potential candidate to be able to exert an effect against LDL oxidation inside the organism.

Those peptides that remain at least partially without being degraded by extracellular peptidases (P2, P3, P4, P5, P6, P8, P9 and P10), when present in the intestinal lumen, could help to maintain the redox balance of the cells of the intestinal mucosa. The peptides with high ORAC capacity could exert a direct effect of neutralization of ROS in the intestinal lumen; in this sense, P2 and P1 would be the most active. All these peptides, except P8 and P9, have showed an effect on the decrease of intracellular ROS, and some other effects related to the antioxidant state of cells, which could be triggered by the presence of the peptide inside the cell or by the activation of some signal by interaction with the plasma membrane. P2 was the only one that did not present any degree of absorption, neither the original molecule, nor any of its hydrolysis products. However, this peptide had shown activity against intracellular ROS. These facts had two possible explanations: 1) P2 enters the cell and inside the cell it is completely degraded so it does not appear in the basolateral chamber; or 2) P2 does not enter the cell but interacts with the plasma membrane and triggers some ROS reduction mechanism.

5. Conclusions

Taking into account that the antioxidant mechanisms of plant protein-derived peptides are not fully understood at the molecular level and that the antioxidant activity depends on the structure of peptides, an analysis of amino acids promoting antioxidant activity was made. It revealed that the presence of some aromatic amino acid (W or Y) and at least one acidic amino acid (E or D) could collaborate with the antioxidant activity. Additionally, the sequence of peptides allowed to evaluate bulk properties as the hydrophobicity and, finally, the modelling of the three-dimensional structure and the simulation of their molecular dynamics behaviour conducted to conjecture the relationships with the bioactivity. The physicochemical properties (global charges, ASA surfaces among others) as well as the cell interaction characteristics of amaranth peptides could be then related with their antioxidant activity. In conclusion, the results described here are the first step to design a quantitative structure–activity relationship (QSAR) between structures and *in vitro*, *ex-vivo* and cellular activities.

In addition, peptides showed different abilities to cross the intestinal barrier. According to this, some peptides could exert their effect almost exclusively in the intestinal level (in the lumen and/or intracellularly) while others, can cross the cell monolayer entering the general circulation. For those peptides that generated other products by the action of the brush border peptidases, the question is raised about the activity of the new molecules, both at the level of the intestinal mucosa and at the systemic level for those that manage to be absorbed. This information is extremely relevant when considering the use of these peptides as nutraceuticals.

The present study demonstrated that amaranth peptides generated by simulated gastrointestinal digestion can exert their antioxidant effect through different mechanisms which could be dependent on their physicochemical/structural characteristics according to the environment as well as on the diverse behaviours of modification and/or passage through the intestinal cells.

Declaration of Competing Interest

The authors declare that they have no known competing financial interests or personal relationships that could have appeared to influence

the work reported in this paper.

Appendix A. Supplementary data

Supplementary data to this article can be found online at https://doi.org/10.1016/j.fochms.2021.100053.

References

Agyei, D., Bambarandage, E., & Udenigwe, C. C. (2018). The role of bioinformatics in the discovery of bioactive peptides. *Reference Module in Food Science, 1–9*, Elsevier. https://doi.org/10.1016/B978-0-08-100596-5.21863-5

Aito-Inoue, M., Lackeyram, D., Fan, M. Z., Sato, K., & Mine, Y. (2007). Transport of a tripeptide, Gly-Pro-Hyp, across the porcine intestinal brush-border membrane. *Journal of Peptide Science, 13*(7), 468–474. https://doi.org/10.1002/(ISSN)1099-138710.1002/psc.v13:710.1002/psc.870

Azad, M., & Wright, G. (2012). Determining the mode of action of bioactive compounds. *Bioorganic and Medicinal Chemistry, 20*(6), 1929–1939. https://doi.org/10.1016/j.bmc.2011.10.088

Bagag, A., Jault, J.-M., Sidahmed-Adrar, N., Réfrégiers, M., Giuliani, A., Le Naour, F., & Lisacek, F. (2013). Characterization of hydrophobic peptides in the presence of detergent by photoionization mass spectrometry. *PLoS ONE, 8*(11), e79033. https://doi.org/10.1371/journal.pone.0079033

Cid, H., Bunster, M., Canales, M., & Gazitúa, F. (1992). Hydrophobicity and structural classes in proteins. *Protein Engineering, Design and Selection, 5*(5), 373–375. https://doi.org/10.1093/protein/5.5.373

Cilla, A., Rodrigo, M. J., Zacarías, L., De Ancos, B., Sánchez-Moreno, C., Barberá, R., & Alegría, A. (2018). Protective effect of bioaccessible fractions of citrus fruit pulps against H2O2-induced oxidative stress in Caco-2 cells. *Food Research International, 103*, 335–344.

Egusa Saiga, A., & Nishimura, T. (2013). Antioxidative properties of peptides obtained from porcine myofibrillar proteins by a protease treatment in an Fe (II)-induced aqueous lipid peroxidation system. *Bioscience, Biotechnology, and Biochemistry, 77*(11), 2201–2204. https://doi.org/10.1271/bbb.130369

Finley, J., Kong, A., Hintze, K., Jeffery, E., Ji, L., & Lei, X. (2011). Antioxidants in foods: State of the science important to the food industry. *Journal of Agricultural and Food Chemistry, 59*(13), 6837–6846. https://doi.org/10.1021/jf2013875

Gallego, M., Mora, L., & Toldrá, F. (2018). Characterisation of the antioxidant peptide AEEEYPDL and its quantification in Spanish dry cured ham. *Food Chemistry, 258*, 8–15. https://doi.org/10.1016/j.foodchem.2018.03.035

García Fillería, S., & Tironi, V. (2017). Prevention of *in vitro* oxidation of low density lipoproteins (LDL) by amaranth peptides released by gastrointestinal digestion. *Journal of Functional Foods, 34*, 197–206. https://doi.org/10.1016/j.jff.2017.04.032

García Fillería, S., & Tironi, V. (2021). Intracellular antioxidant activity and intestinal absorption of amaranth peptides released using simulated gastrointestinal digestion with Caco-2 TC7 cells. *Food Bioscience, 41*(4), Article 101086. https://doi.org/10.1016/j.fbio.2021.101086

Guidotti, G., Brambilla, L., & Rossi, D. (2017). Cell-penetrating peptides: From basic research to clinics. *Trends in Pharmacological Sciences, 38*(4), 406–424. https://doi.org/10.1016/j.tips.2017.01.003

Gupta, S., Kapoor, P., Chaudhary, K., Gautam, A., Kumar, R., Raghava, G. P. S., & Patterson, R. L. (2013). *In Silico* approach for predicting toxicity of peptides and proteins. *PLoS ONE, 8*(9), e73957. https://doi.org/10.1371/journal.pone.0073957

Hernández-Ledesma, B., Amigo, L., Recio, I., & Bartolomé, B. (2007). ACE-inhibitory and radical-scavenging activity of peptides derived from β-lactoglobulin f(19–25). Interactions with ascorbic acid. *Journal of Agricultural and Food Chemistry, 55*(9), 3392–3397. https://doi.org/10.1021/jf063427j

Holton, T., Vijayakumar, V., & Khaldi, N. (2013). Bioinformatics: Current perspectives and future directions for food and nutritional research facilitated by a Food-Wiki database. *Trends in Food Science and Technology, 34*(1), 5–17. https://doi.org/10.1016/j.tifs.2013.08.009

Jiménez, S., Gascón, S., Luquin, A., Laguna, M., Ancin-Azpilicueta, C., Rodríguez-Yoldi, M. J., & Pintus, G. (2016). Rosa canina extracts have antiproliferative and antioxidant effects on Caco-2 human colon cancer. *Plos One, 11*(7), e0159136. https://doi.org/10.1371/journal.pone.0159136

Ketnawa, S., Wickramathilaka, M., & Liceaga, A. (2018). Changes on antioxidant activity of microwave-treated protein hydrolysates after simulated gastrointestinal digestion:

Purification and identification. *Food Chemistry, 254*, 36–46. https://doi.org/10.1016/j.foodchem.2018.01.133

Kyte, J., & Doolittle, R. (1982). A simple method for displaying the hydropathic character of a protein. *Journal of Molecular Biology, 157*(1), 105–132. https://doi.org/10.1016/0022-2836(82)90515-0

Leong, S. Y., Burritt, D. J., Hocquel, A., Penberthy, A., & Oey, I. (2017). The relationship between the anthocyanin and vitamin C contents of red-fleshed sweet cherries and the ability of fruit digests to reduce hydrogen peroxide-induced oxidative stress in Caco-2 cells. *Food Chemistry, 227*, 404–412.

Li, Y., & Li, B. (2013). Characterization of structure-antioxidant activity relationship of peptides in free radical systems using QSAR models: Key sequence positions and their amino acid properties. *Journal of Theoretical Biology, 318*, 29–43. https://doi.org/10.1016/j.jtbi.2012.10.029

López-Alarcón, C., & Denicola, A. (2013). Evaluating the antioxidant capacity of natural products: A review on chemical and cellular-based assays. *Analytica Chimica Acta, 763*, 1–10. https://doi.org/10.1016/j.aca.2012.11.051

Nardo, A. E., Suárez, S., Quiroga, A. V., & Añón, M. C. (2020). Amaranth as a source of antihypertensive peptides. *Frontiers in Plant Science, 11*, Article 578631. https://doi.org/10.3389/fpls.2020.578631

Nwachukwu, I. D., & Aluko, R. E. (2019). Structural and functional properties of food protein-derived antioxidant peptides. *Journal of Food Biochemistry, 43*(1), e12761. https://doi.org/10.1111/jfbc.12761

O'Sullivan, A. M., O'Callaghan, Y. C., O'Grady, M. N., Queguineur, B., Hanniffy, D., Troy, D. J., … O'Brien, N. M. (2012). Assessment of the ability of seaweed extracts to protect against hydrogen peroxide and tert-butyl hydroperoxide induced cellular damage in Caco-2 cells. *Food Chemistry, 134*(2), 1137–1140. https://doi.org/10.1016/j.foodchem.2012.02.205

Orsini Delgado, M. C., Galleano, M., Añón, M. C., & Tironi, V. A. (2015). Amaranth peptides from simulated gastrointestinal digestion: Antioxidant activity against reactive species. *Plant Foods for Human Nutrition, 70*(1), 27–34. https://doi.org/10.1007/s11130-014-0457-2

Orsini Delgado, M. C., Nardo, A., Pavlovic, M., Rogniaux, H., Añón, M. C., & Tironi, V. A. (2016). Identification and characterization of antioxidant peptides obtained by gastrointestinal digestion of amaranth proteins. *Food Chemistry, 197*, 1160–1167. https://doi.org/10.1016/j.foodchem.2015.11.092

Pan, M., Huo, Y., Wang, C., Zhang, Y., Dai, Z., & Li, B. (2019). Positively charged peptides from casein hydrolysate show strong inhibitory effects on LDL oxidation and cellular lipid accumulation in Raw264.7 cells. *International Dairy Journal, 91*, 119–128.

Park, S. J., Sharma, A., & Lee, H. J. (2020). A review of recent studies on the antioxidant activities of a third-millennium food: *Amaranthus* spp. *Antioxidants, 9*(12), 1–22. https://doi.org/10.3390/antiox9121236

Phongthai, S., D'Amico, S., Schoenlechner, R., Homthawornchoo, W., & Rawdkuen, S. (2018). Fractionation and antioxidant properties of rice bran protein hydrolysates stimulated by *in vitro* gastrointestinal digestion. *Food Chemistry, 240*, 156–164. https://doi.org/10.1016/j.foodchem.2017.07.080

Quirós, A., Dávalos, A., Lasunción, M. A., Ramos, M., & Recio, I. (2008). Bioavailability of the antihypertensive peptide LHLPLP: Transepithelial flux of HLPLP. *International Dairy Journal, 18*(3), 279–286. https://doi.org/10.1016/j.idairyj.2007.09.006

Regazzo, D., Mollé, D., Gabai, G., Tomé, D., Dupont, D., Leonil, J., & Boutrou, R. (2010). The (193–209) 17-residues peptide of bovine β-casein is transported through Caco-2 monolayer. *Molecular Nutrition & Food Research, 54*(10), 1428–1435. https://doi.org/10.1002/mnfr.v54:1010.1002/mnfr.200900443

Ryu, B., Himaya, S., Qian, Z., Lee, S., & Kim, S. (2011). Prevention of hydrogen peroxide-induced oxidative stress in HDF cells by peptides derived from seaweed pipefish, Syngnathus schlegeli. *Peptides, 32*(4), 639–647. https://doi.org/10.1016/j.peptides.2011.01.009

Savoie, L., Agudelo, R. A., Gauthier, S. F., Marin, J., & Pouliot, Y. (2005). *In vitro* determination of the release kinetics of peptides and free amino acids during the digestion of food proteins. *Journal of AOAC International, 88*, 935–948. https://doi.org/10.1093/jaoac/88.3.935

Stothard, P. (2000). The Sequence Manipulation Suite: JavaScript programs for analyzing and formatting protein and DNA sequences. *Biotechniques, 28*(6), 1102–1104. https://doi.org/10.2144/00286ir01

Turco, L., Catone, T., Caloni, F., Consiglio, E. D., Testai, E., & Stammati, A. (2011). Caco-2/TC7 cell line characterization for intestinal absorption: How reliable is this *in vitro* model for the prediction of the oral dose fraction absorbed in human? *Toxicology in vitro, 25*(1), 13–20. https://doi.org/10.1016/j.tiv.2010.08.009

Wang, L., Ding, L., Wang, Y., Zhang, Y., & Liu, J. (2015). Isolation and characterization of in vitro and cellular free radical scavenging peptides from corn peptide fractions. *Molecules, 20*(2), 3221–3237.

Wang, B., Wang, C., Huo, Y., & Li, B. (2016). The absorbates of positively charged peptides from casein show high inhibition ability of LDL oxidation *in vitro*: Identification of intact absorbed peptides. *Journal of Functional Foods, 20*, 380–393. https://doi.org/10.1016/j.jff.2015.11.012

Wen, C., Zhang, J., Zhang, H., Duan, Y., & Ma, H. (2020). Plant protein-derived antioxidant peptides: Isolation, identification, mechanism of action and application in food systems: A review. *Trends in Food Science and Technology, 105*, 308–322. https://doi.org/10.1016/j.tifs.2020.09.019

Xu, F., Wang, L., Ju, X., Zhang, J., Yin, S., Shi, J., … Yuan, Q. (2017). Transepithelial transport of YWDHNNPQIR and its metabolic fate with cytoprotection against oxidative stress in human intestinal Caco-2 cells. *Journal of Agricultural and Food Chemistry, 65*(10), 2056–2065. https://doi.org/10.1021/acs.jafc.6b04731

Zou, T., He, T., Li, H., Tang, H., & Xia, E. (2016). The structure-activity relationship of the antioxidant peptides from natural proteins. *Molecules, 21*(1), 1–14. https://doi.org/10.3390/molecules21010072